Stable radical cores: a key for bipolar charge transport in glass forming carbazole and indole derivatives.

Sonia Castellanos[†], Valentas Gaidelis[‡], Vygintas Jankauskas[‡], Juozas V. Grazulevicius[§], Enric Brillas[□], Francisco López-Calahorra[□], Luis Juliá[†]*, Dolores Velasco[□]*

Contribution from the Departament de Química Biològica i Modelització Molecular, Institut de Química Avançada de Catalunya (CSIC), 08034 Barcelona, Departament de Química Orgànica, Universitat de Barcelona, 08028 Barcelona, Departament de Química Física, Universitat de Barcelona, 08028 Barcelona, Spain, Department of Solid State Electronics, Vilnius University, LT-10222 Vilnius, Lithuania, Department of Organic Technology, Kaunas University of Technology, 3028 Kaunas, Lithuania.

Supporting Information

Table of contents **page**

[†] Institut de Química Avançada de Catalunya (CSIC)
[‡] University of Vilnius
[§] University of Kaunas
[□] Departament de Química Física, Universitat de Barcelona
[□] Departament de Química, Orgànica Universitat de Barcelona

Table. *Electrochemical potential values[a] in volts for radicals **1**, **2**, and **3***

	E^{o}_{r}/V	E_{r}^{onset}	E^{o}_{o}/V	E_{o}^{onset}
1	-0.52	-0.44	1.03	0.98
2	-0.50	-0.48	1.00	0.92
3	-0.51	-0.42	1.27	1.22

[a]Potential values versus SCE (saturated calomel electrode)

The **electron affinity** (EA) and **ionization potential** (IP) values of radicals were estimated on the basis of the referente energy level of ferrocene (4.8 eV below the vacuum level) according to the formula

$$EA/IP = 4.8 + E^{onset} - E^{o}(Fc/Fc^{+}) \text{ eV},$$

Where E^{onset} are the onset potentials for reduction and oxidation of radicals *versus* SCE, respectively, and where $E^{o}(Fc/Fc^{+}) = 0.16$ V is the redox potential for the oxidation of ferrocene *versus* SCE.

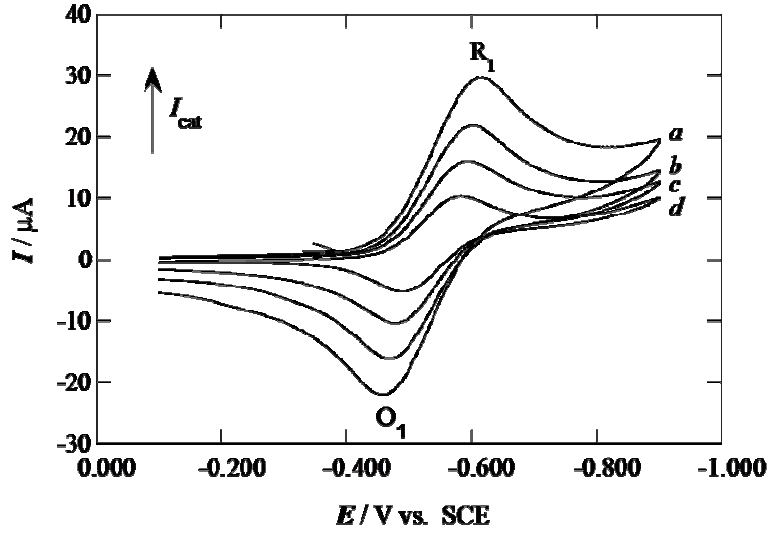

Figure S1. Cyclic voltammograms corresponding to the reduction of a CH_2Cl_2 solution of **2** (1 mM) with TBAP 0.1 M on Pt at 25 ºC. Initial and final potential -0.200 V; reversal potential -0.900 V. Scan rate: (a) 200, (b) 100, (c) 50, (d) 20 mV s^{-1}.

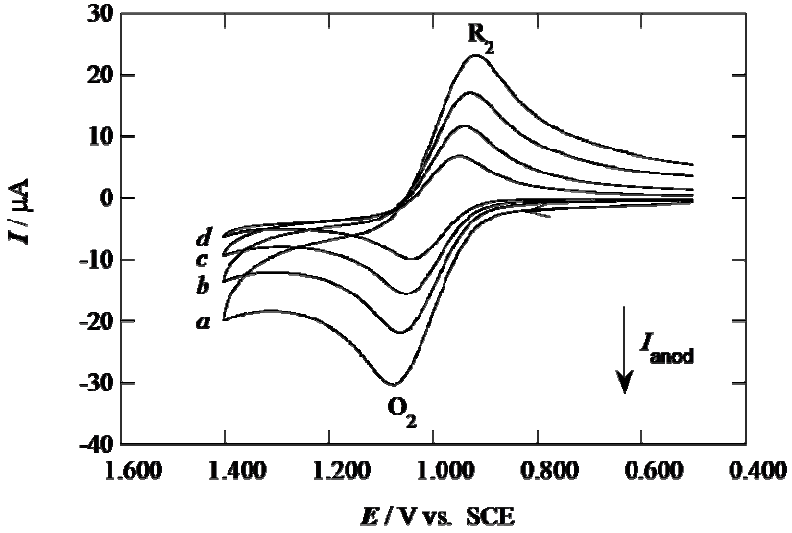

Figure S2. Cyclic voltammograms corresponding to the oxidation of a CH_2Cl_2 solution of **2** (1 mM) with TBAP 0.1 M on Pt at 25 ºC. Initial and final potential 0.500 V; reversal potential 1.400 V. Scan rate: (a) 200, (b) 100, (c) 50, (d) 20 mV s^{-1}.

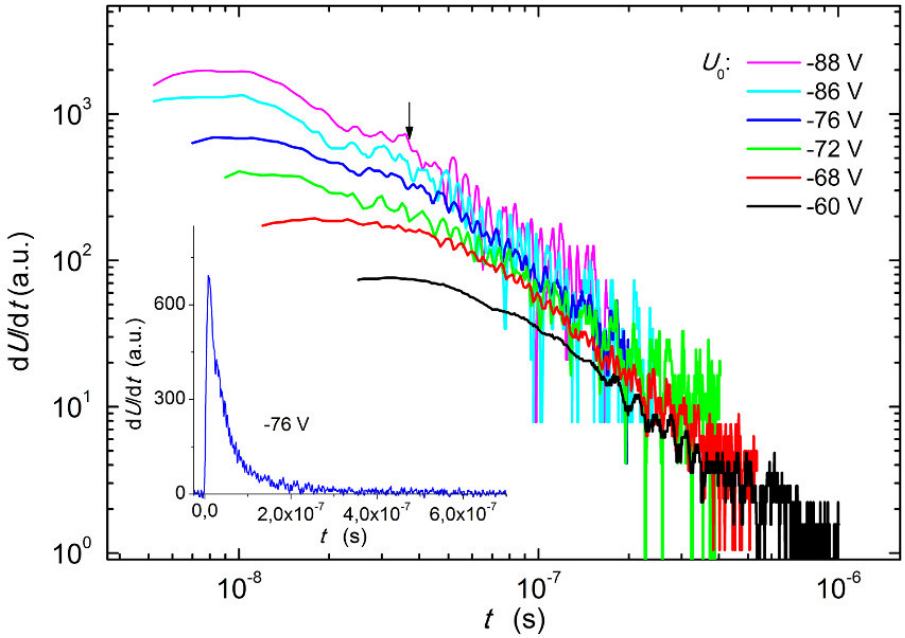

Figure S3. Logarithmic surface potential decay of a layer of **1** (1.5 μm) for negative corona charging. Inserts are the lineal surface potential decays at the given initial corona charging.

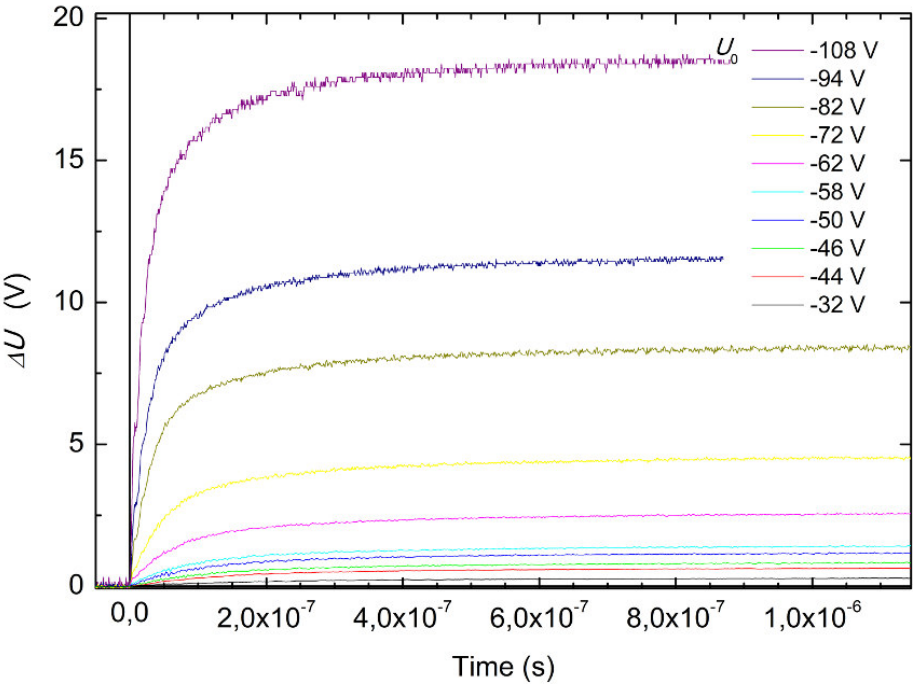

Figure S4. Integral of the surface potential decay of a layer of **1** (1.5 μm) for negative corona charging.

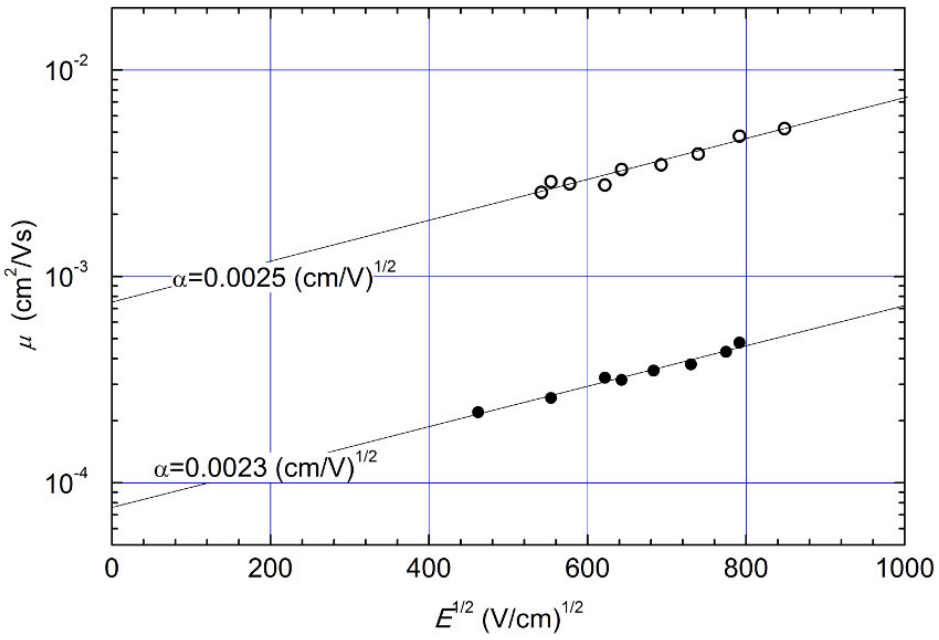

Figure S5. Electron (white circles) and hole (black circles) mobility values vs. electric field of layers of a layer of **1**.

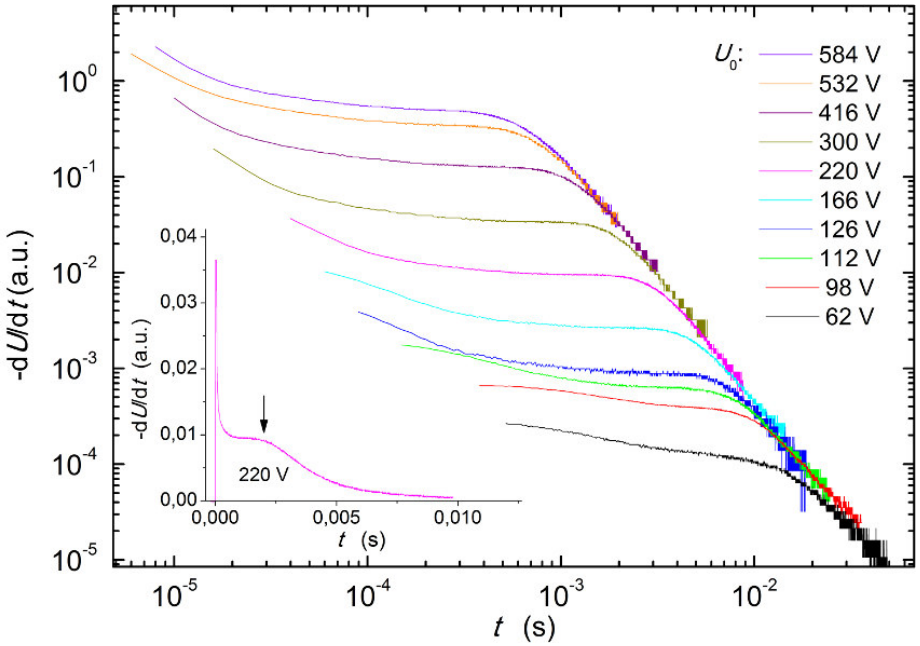

Figure S6. Logarithmic surface potential decay of a layer of **1**:PCZ blend (7 μm) for positive corona charging. Inserts are the lineal surface potential decays at the given initial corona charging.

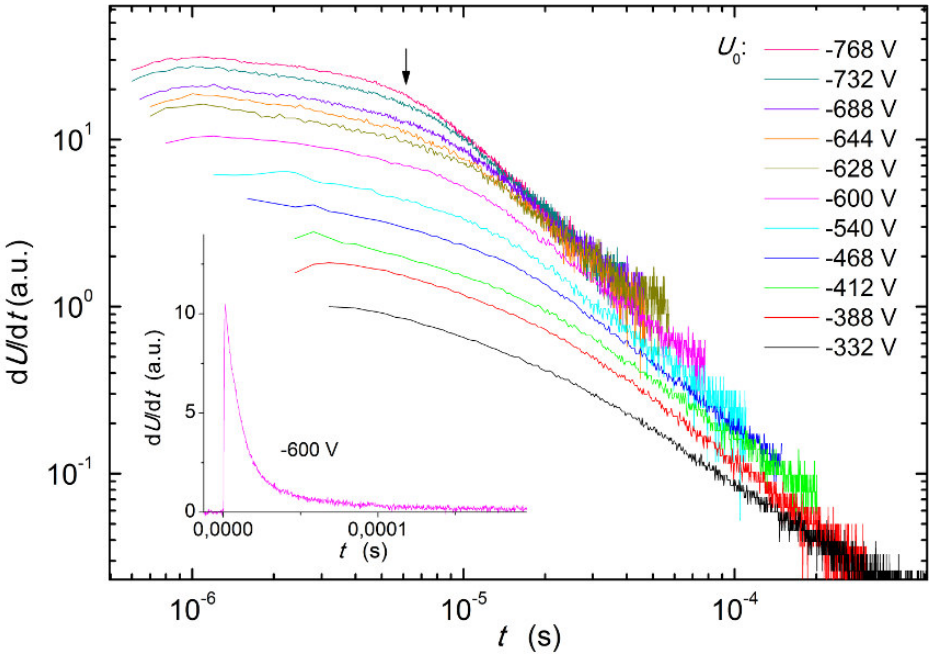

Figure S7. Logarithmic surface potential decay of a layer of **1**:PCZ blend (7 μm) for negative corona charging. Inserts are the lineal surface potential decays at the given initial corona charging.

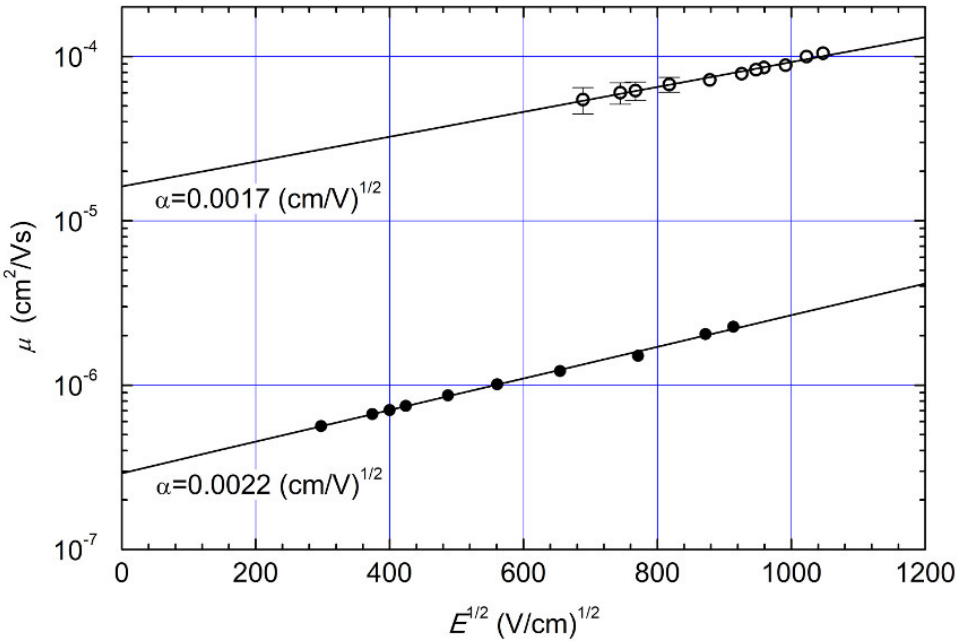

Figure S8. Electron (white circles) and hole (black circles) mobility values vs. electric field of layers of the blend **1**:PCZ.

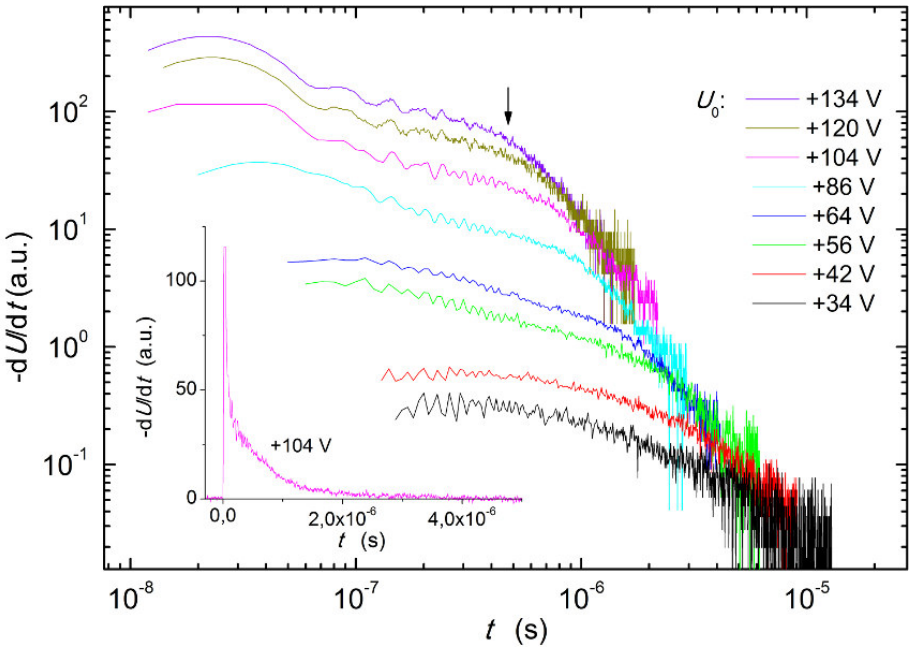

Figure S9. Logarithmic surface potential decay of a layer of **2** (2.1 µm) lend for positive corona charging. Inserts are the lineal surface potential decays at the given initial corona charging.

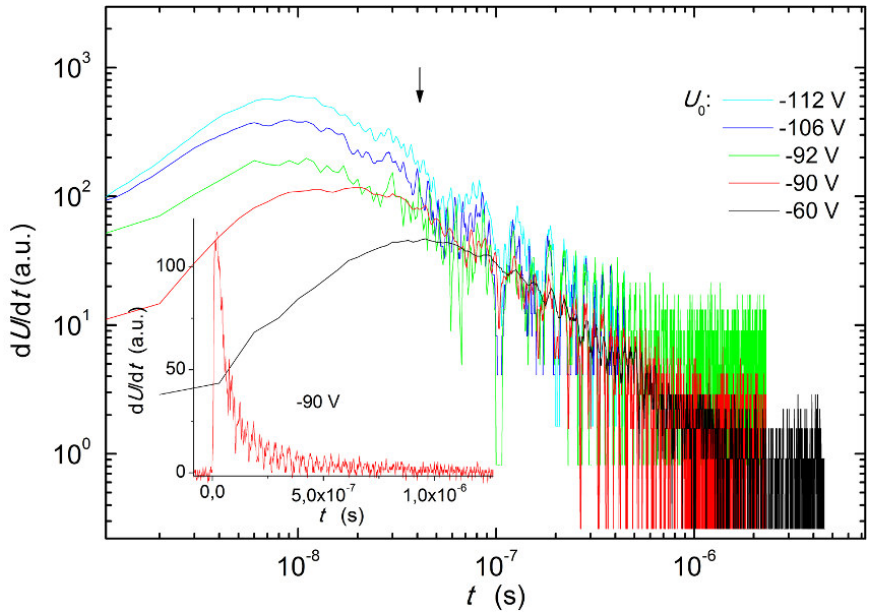

Figure S10. Logarithmic surface potential decay of a layer of **2** (2.1 µm) lend for negative corona charging. Inserts are the lineal surface potential decays at the given initial corona charging.

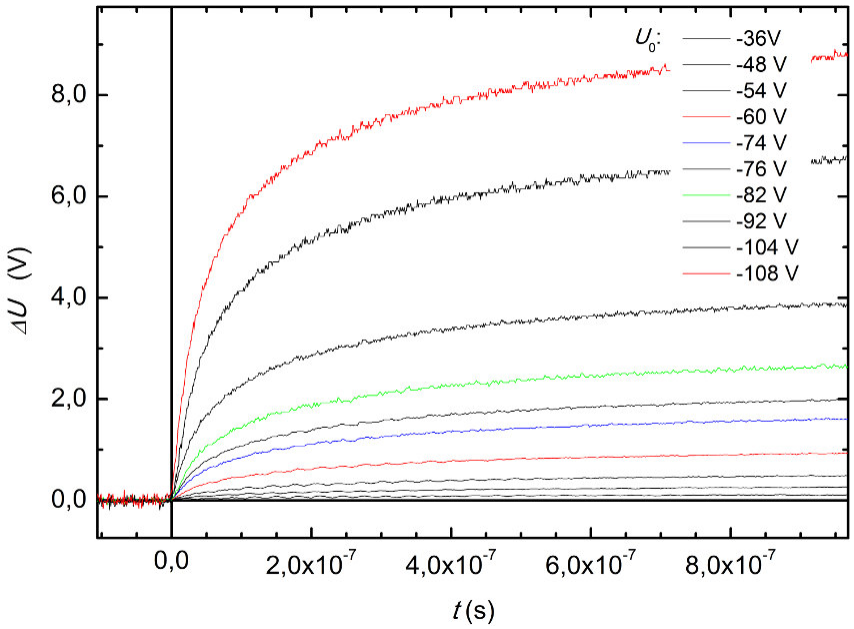

Figure S11 Integral of the surface potential decay of a layer of **2** (2.1 μm) lend for negative corona charging.

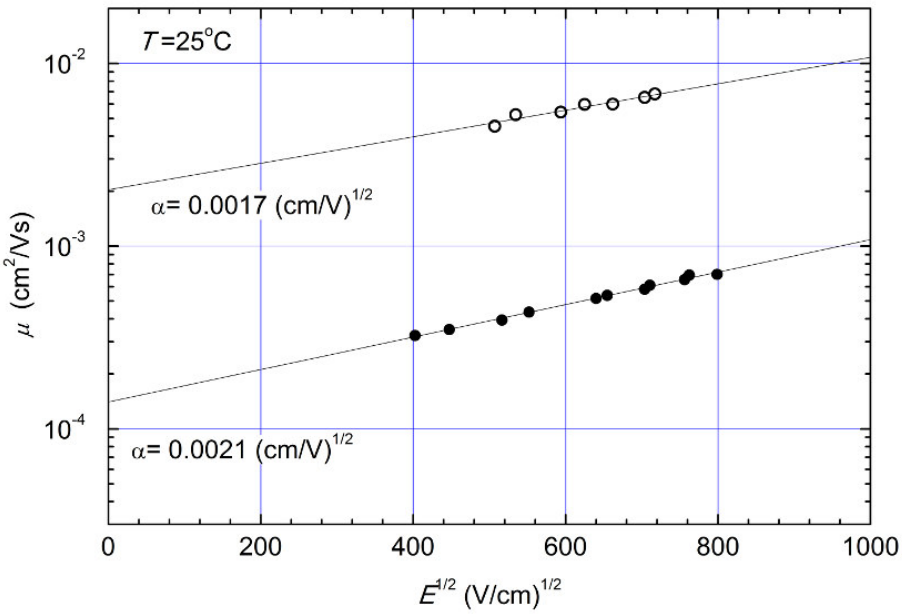

Figure S12. Electron (white circles) and hole (black circles) mobility values vs. electric field of layers of pure material **2**.

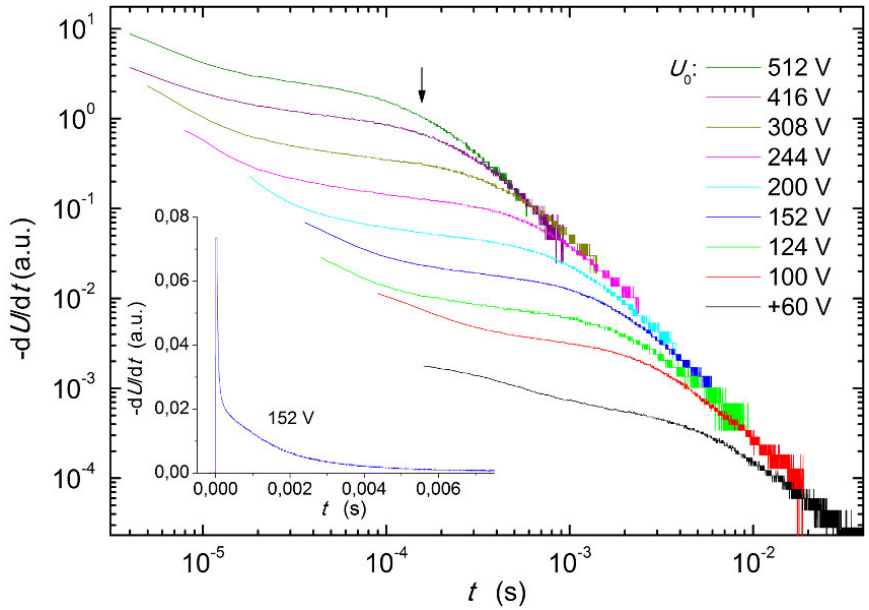

Figure S13. Logarithmic surface potential decay of a layer of **2**:PCZ blend (4.8 μm) for positive corona charging. Inserts are the lineal surface potential decays at the given initial corona charging.

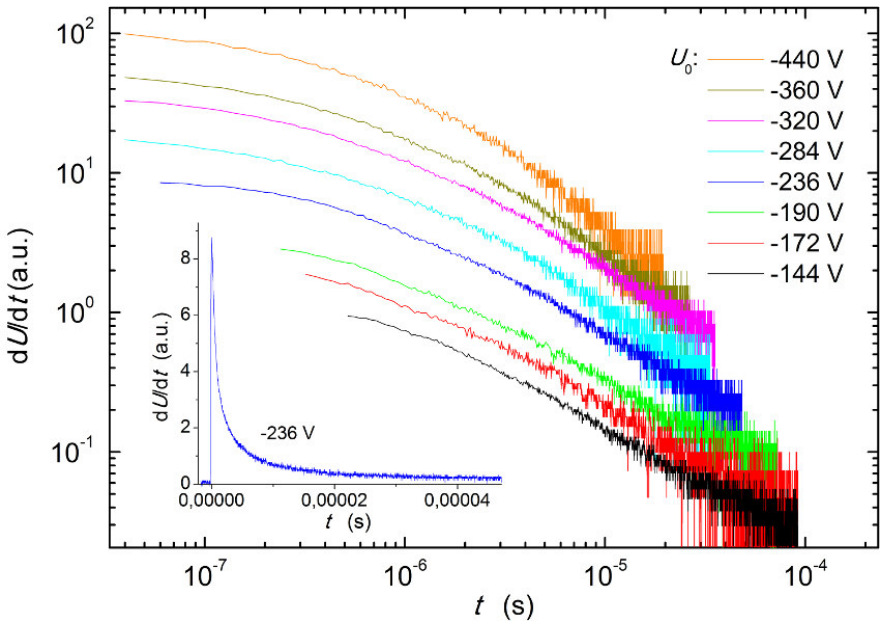

Figure S14. Logarithmic surface potential decay of a layer of **2**:PCZ blend (4.8 μm) for negative corona charging. Inserts are the lineal surface potential decays at the given initial corona charging.

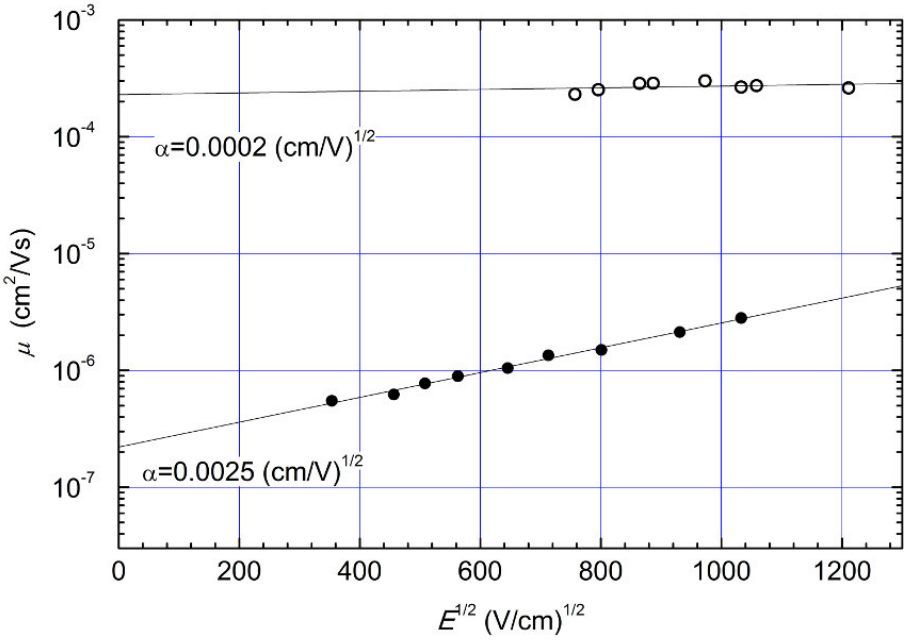

Figure S15. Electron (white circles) and hole (black circles) mobility values vs. electric field of layers of the blend **2**:PCZ.

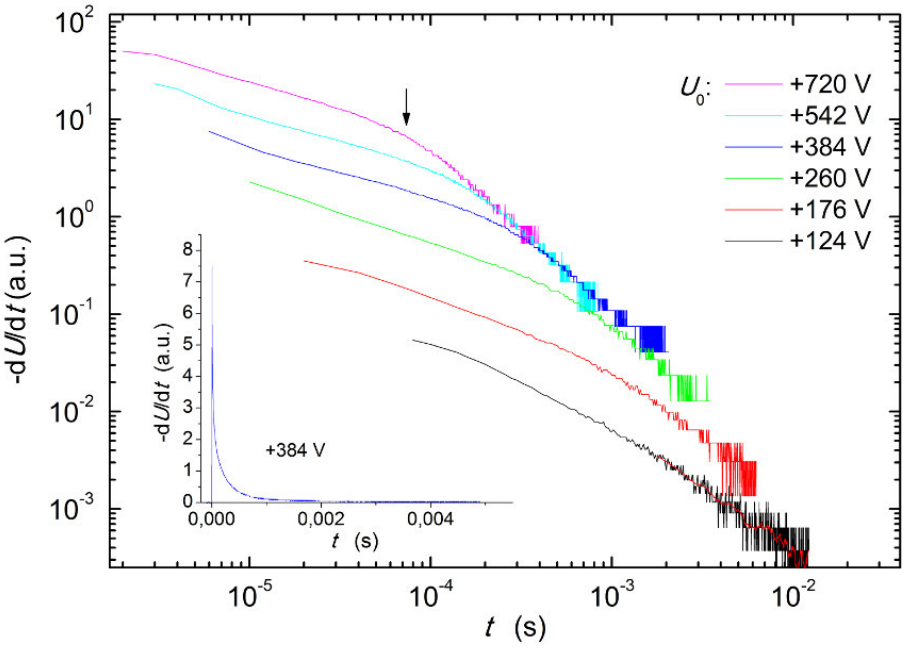

Figure S16. Logarithmic surface potential decay of a layer of **3**:PCZ blend (6 μm) for positive corona charging. Inserts are the lineal surface potential decays at the given initial corona charging.

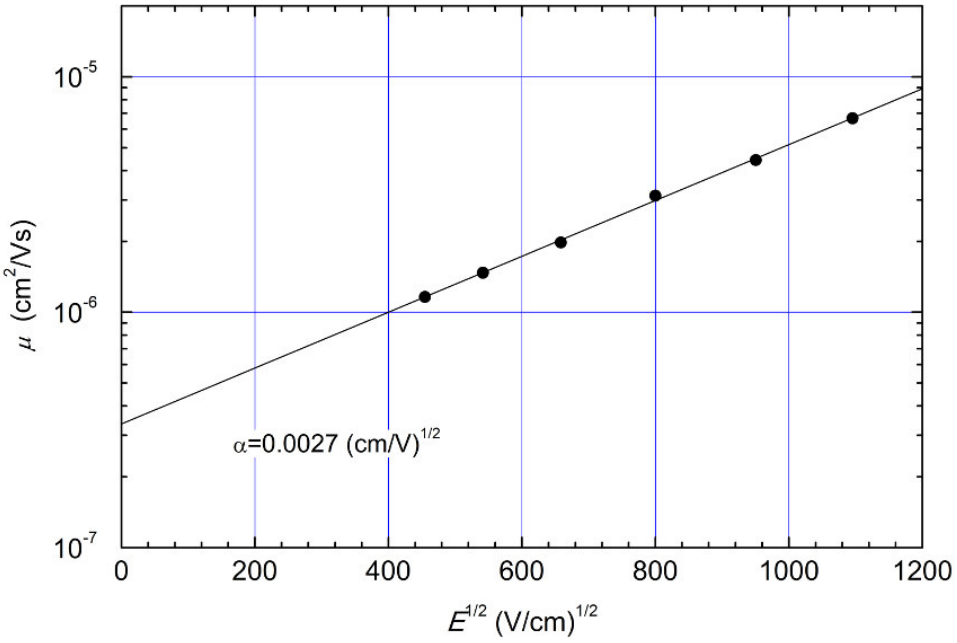

Figure S17. Hole mobility values vs. electric field of layers of the blend **3**:PCZ.